Available online at www.sciencedirect.com
SCIENCE DIRECT®

Journal of the European Ceramic Society 24 (2004) 1935–1939
www.elsevier.com/locate/jeurceramsoc

Combustion synthesis and the influence of precursor packing on the sintering properties of LCC nanopowders

K. Zupan*, M. Marinšek, S. Pejovnik, J. Maček, K. Zore

Faculty of Chemistry and Chemical Technology, University of Ljubljana Aškerčeva 5, 1000 Ljubljana, Slovenia

Abstract

The sintering characteristics of calcium-substituted lanthanum chromite powders (LCC) prepared via the citrate-nitrate combustion route were examined. The effects of sample packing prior to combustion synthesis and (La + Ca)/Cr cation ratios were studied in terms of the degree of reaction conversion and agglomeration of the nanoparticles obtained. The difference in sintering behaviour of samples milled for 5 and 60 min indicates that the sintering properties of the samples are not related only to the presence of liquid phase but also to the agglomerate size reduction during milling.

Keywords: Combustion synthesis; Fuel cells; Sintering

1. Introduction

Lanthanum chromite based materials are being widely studied for applications in solid oxide fuel cells (SOFCs) due to their high electrical conductivity and their chemical stability at elevated temperatures. However, applications of pure lanthanum chromite are limited by its poor sinterability in air, which can be improved by partially replacing lanthanum with alkaline earth elements and chromium with zinc, nickel or copper.[1] These doping elements decrease the evaporation of chromium oxide or form a liquid phase with chromite during sintering, and also influence the electrical conductivity.[2] A considerable improvement in the sintering process can result from a small enhancement in the (La + Ca)/Cr cation ratios.[3] A significant influence on sintering can also be achieved by using nonagglomerated reactive powders.[4]

Preparation of complex metal oxides by combustion synthesis has become an important powder preparative technique due to promising results in particle size reduction and the high degree of conversion to reactive powders. The exothermic reaction between fuel and oxidant is accompanied by release of a relatively large volume of gases that prevents formation of hard agglomerates. A comparison of the reactions of mixtures consisting of nitrates and urea or glycine that proceed by explosive combustion with those of the citrate-nitrate gel system revealed that the latter are more controllable due to their smaller exothermal effect. Combustion synthesis can be performed in the thermal explosion mode, where the sample is heated uniformly and reaction occurs almost simultaneously throughout all of the mixture. In the self-propagating mode, the reaction is initiated at one end of the reaction mixture and propagates through the volume in the form of a combustion wave.[5]

The aim of this research was to determine the influence of the packing of the reaction mixture prior to combustion on the combustion mode, the degree of reactant conversion, and the sintering behaviour of stoichiometric and substoichiometric LCC powders prepared via the citrate-nitrate combustion route.

2. Experimental procedures

LCC powders were prepared by a modified citrate/nitrate gel combustion synthesis. The starting substances (analytical reagent grade) for reactive gel preparation were aqueous solutions of $La(NO_3)_3{\cdot}6H_2O$, $Cr(NO_3)_3{\cdot}9H_2O$, $Ca(NO_3)_24H_2O$ and citric acid. All four precursors were mixed together to prepare solutions which were kept over a water bath at 60 °C under vacuum until they transformed into a gel. Samples with nominal compositions $La_{0.7}Ca_{0.3}CrO_3$ and $La_{0.7}Ca_{0.3}Cr_{0.98}O_3$ were prepared by ignition of the corresponding

* Corresponding author.

0955-2219/$ - see front matter © 2003 Elsevier Ltd. All rights reserved.
doi:10.1016/S0955-2219(03)00546-6

citrate nitrate gel. At least two alternative sets of combustion experiments were made for each reaction mixture. The starting material for both sets was prepared in the same way. For the first set the dried gel was milled in an agate mortar and loosely distributed in a ceramic receptacle to an approximate height of 10 mm covering a surface of 20 cm^2. The material for the second set was pressed into pellets of 12 mm radius and 30 mm height using pressures of 17 MPa. Both samples were ignited by the flame of a very small gas burner, either at one end of the dispersed sample layer or on top of the pellet. The details of the technique, for preparation of LCC gels have been described elsewhere.[6] Sample preparation conditions and combustion rates are summarised in Table 1. The initial citrate/nitrate (c/n) molar ratio in all reaction mixtures was 0.18. The products of synthesis were characterized by the X-ray powder diffraction technique using a Philips PW-1710 apparatus. TG analysis was performed on a Netzsch STA 409 apparatus. A Micromeritics Gemini II 2370 was used to determine specific surface areas by the BET method. SEM characterization was carried out on Jeol T300 and the particle size distribution of sample A on a Fritsch Analysette 22 granulometer. Prior to the determination of particle size the samples were milled in isopropanol in an agate ball mill and dispersed in 1% NaCl aqueous solution. Shrinkage during sintering was measured by a Leitz Wetzlar heating microscope. Powders were unaxially pressed at 200 MPa and sintered for 10 h at 1250 or 1300 °C in air. The sintered samples were also examined by optical microscopy.

3. Results and discussion

The rate of the combustion reaction was strongly influenced by the initial c/n molar ratio. The calculated stoichiometric c/n initial molar ratio for the LCC system is 0.28.[7] However, the velocity of propagation of the combustion of citrate/nitrate precursor gels was found to be the highest for lower initial c/n molar ratios.[6] Combustion rates, specific surface areas (SSA) and product crystallite sizes of the samples are given in Table 1. The combustion rates were 9–15 times higher when combustion proceeded in the layer form. The reaction time of precursors B and D was 2 and 3 s, respectively, while it took 25 s for reaction completition of mixtures A and C for the same mass of reacting gel. The combustion reaction mode depends on both the fuel/oxidant ratio and the reaction mixture packing prior to ignition. The combustion reaction proceeded in the thermal explosion mode in the case of sample distribution in the form of a layer, and in the self-sustaining mode for samples shaped into pellet form. In the latter case the products continuously expanded from the reaction zone during combustion.

X-ray analysis of the products after combustion confirmed that all samples had an identical modified cubic lanthanum chromite structure. The presence of a single phase perovskite structure was determined for sample D, while in samples A, B and C traces of the secondary phase $CaCrO_4$ were also found. Products formed from pellets were slightly better crystallized with a crystallite size near 23 nm (determined on the basis of X-ray peak broadening). On the other hand, crystallite sizes in the samples formed by combustion in a layer were calculated to be 13–15 nm. The calculated trend of the crystallite sizes is in good agreement with the measured specific surface areas of the samples. It appears that heat transfer is more uniform throughout the pellets while the effect of escaping gases is probably comparable in both types of reaction mixture packing. Consequently, the higher reaction temperatures and reaction times in the pelletised samples contribute to their better crystallinity.

The thermal behaviour of the samples is strongly dependent on the sample geometry prior to the ignition and chromium stoichiometry (Fig. 1). Total mass loss in the samples after synthesis was greater when the reaction was performed in layer form for chromium-depleted samples. Minor mass losses of 1.5 and 2.3% were

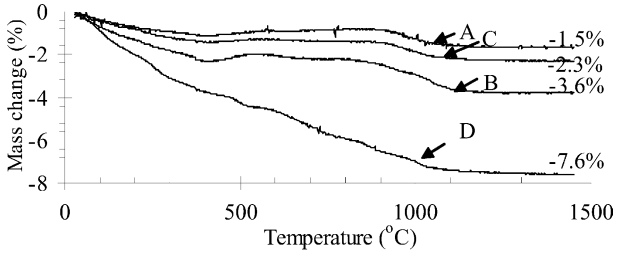

Fig. 1. TG curves of samples after combustion synthesis.

Table 1
Preparation conditions, combustion rates, specific surface areas and crystallite sizes of all samples

Sample	Composition	Sample packing prior to combustion	Combustion rate (g/s)	SSA (m^2/g)	$d_{(100)}$ (nm)	$d_{(110)}$ (nm)
A	$La_{0.7}Ca_{0.3}CrO_3$	Pellet	0.6	11.9	23.4	23.3
B	$La_{0.7}Ca_{0.3}CrO_3$	Loose packed layer	9.0	12.9	15.3	15.1
C	$La_{0.7}Ca_{0.3}Cr_{0.98}O_3$	Pellet	0.6	11.6	23.2	23.2
D	$La_{0.7}Ca_{0.3}Cr_{0.98}O_3$	Loose packed layer	5.5	17.7	13.1	13.1

observed in the case of pelletised samples, while mass losses of 3.6 and 7.6% were determined for in-layer prepared samples due to the lower degree of conversion. The shorter reaction time at reaction temperature for the layer combusted samples was also confirmed by a higher mass loss (~1.5%) in the temperature region from 800 to 1160 °C, while for the pelletised samples (A and C) the lower mass loss of 0.8% in the same temperature interval indicated that during synthesis dissolution of $CaCrO_4$ into the perovskite occurred. The weight loss in all samples near 1050 °C was probably due to melting of the remaining nonperovskite phase, followed by further dissolution of calcium into the perovskite.[8] Mass losses in the temperature range from 25 to 750 °C observed in the chromium-depleted sample D are probably due to the formation of oxide phases like La_2O_3 during synthesis, which then easily hydrate in moist air at room temperature,[3] as well as some removal of organic residuals.

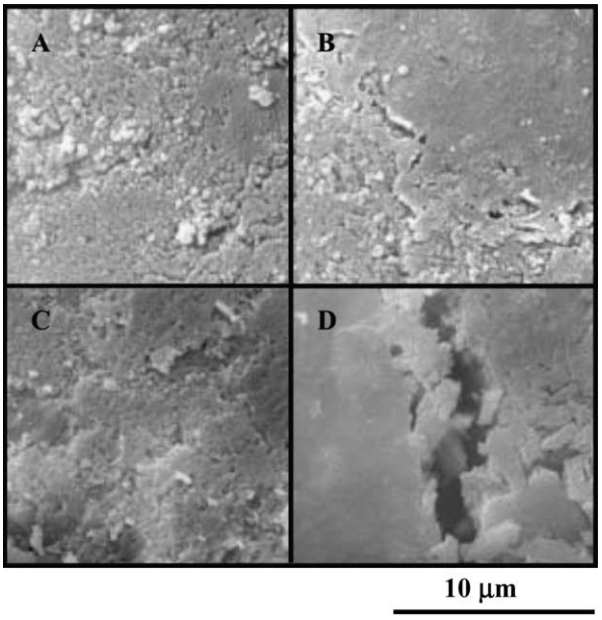

Fig. 2. SEM micrographs of samples (A–D) pressed into tablets at 300 MPa.

SEM micrographs of the samples pressed at 300 MPa are shown in Fig. 2. Individual particles are bound into agglomerates of different sizes and shapes. Chromium-depleted sample D prepared in a loose packed layer differs considerably from samples A, B and C. Sample B is composed of dense agglomerates and less dense regions, while sample D possesses large voids in the green structure. The powder morphology of the product is very dependent on the reaction mixture geometry and the number of contacts between gel particles. As compared with other samples, pellet formed samples A and C exhibit considerably less porous structures and more homogeneous particle arrangements. The thermal explosion mode in layer formed samples is the reason for the nonuniform structure. In the chromium-depleted samples more liquid phase should form[9] which is a plausible reason for hard agglomerate formation during synthesis and large cracks resulting after pressure application.

The average particle sizes d_{50} and standard deviations 2σ versus milling time for sample A are given in Table 2. The average particle size d_{50} decreases markedly in the first 60 min of milling. During further milling d_{50} and 2σ change only slightly. Taking into consideration these

Table 2
Average particle size d_{50} and standard deviation 2σ versus milling time for sample A

Milling time (min)	1	5	30	60	120	180	240	300
d_{50} (μm)	5.15	4.63	2.37	1.61	1.42	1.28	1.11	1.13
2σ (μm)	7.77	7.28	3.48	2.38	1.98	1.74	1.40	1.47

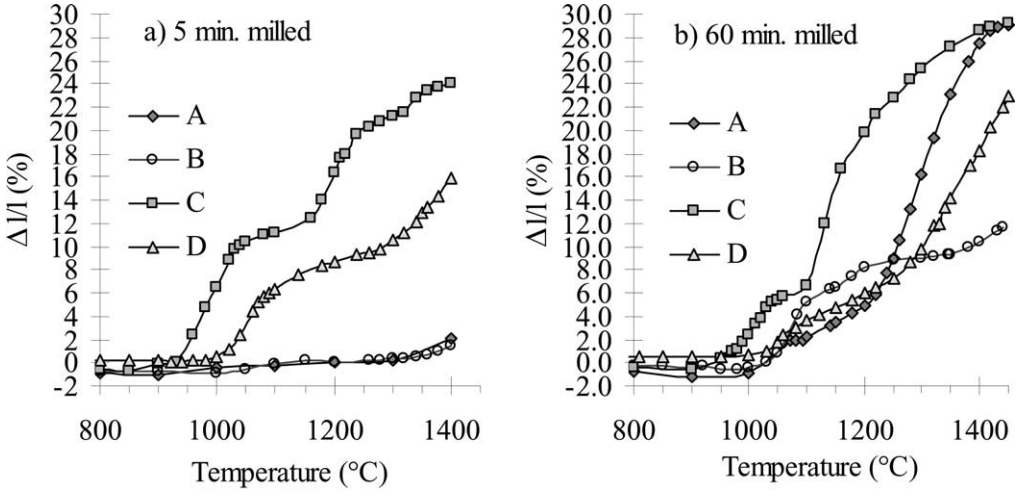

Fig. 3. Relative linear shrinkage versus temperature of milled samples.

results, all samples were milled for 5 and 60 min and subsequently their sintering properties were compared.

Sintering curves of samples (milled 5 or 60 min in an agate mill and unaxially pressed at 70 MPa) are shown in Fig. 3. According to the results shown in Fig. 3a the process of shrinkage of samples C and D occurred in two steps initiated at 920 and 980 °C, respectively. In the case of 5 min milled samples A and B there was no evidence of densification during heating up to 1400 °C. Comparison of the sintering behaviour of samples milled for 5 and 60 min revealed an inflection at 1060 °C, probably associated with the melting of the $CaCrO_4$ secondary phase[8] and followed by a second shrinkage event that started at 1100 °C. This process is most evident in the case of sample A. The densification of sample A in the second step is associated with effective agglomerate size reduction during milling and an easier liquid phase penetration along the grain borders.[10] A similar effect was noticed in chromium-deficient sample C, where a second sintering event for the 60 min milled sample started at a temperature 60 °C lower than for the 5 min milled one. Furthermore, the second densification step increased at the expense of the first shrinkage event. The sinterability of the samples B and D is not essentially improved during milling due to their inhomogeneous structure and lower degree of reactant conversion.

Some data on the sintering behaviour of the samples are summarised in Table 3. The green calculated densities of samples varied from 2.16 to 2.82 g/cm^3 and are higher for the pellet formed samples. The relatively high density archived for chromium-depleted sample C (94% of theoretical density TD) is due to the fact that a lower temperature is required for liquid promoted sintering. As expected from the sintering behaviour shown in Fig. 3, the sintered density of sample A is markedly improved if the sample is milled for 60 min prior to sintering at 1250 °C. The relatively higher density of sample A reflects the differences in the burning process of the precursor in the pelletised form over combustion in a loose packed layer. The presence and subsequent melting of the second phase became as effective as in chromium-depleted sample C after agglomerate size diminution. The measured mass changes during the sintering are in good agreement with the TG analysis data for all samples.

Microstructures of the sintered and polished samples are shown in Fig. 4. Initially layer formed samples (B, D) after 60 min of milling and subsequent sintering exhibited less dense structures at a magnification of 100 than initially pelletised samples (A, C). The high shrinkage in of samples A and C and their high relative densities (93% of the theoretical value) result in a rather small degree of porosity. Heterogeneous pore size

Table 3
Sintering conditions, calculated densities and relative mass changes for milled samples sintered for 10 h

Sample	Sintering temperature (°C)	Milling time (min)	ρ_{green} (g/cm^3)	$\rho_{sinter.}$ (g/cm^3)	$\rho_{X\text{-}ray}$ (g/cm^3)	$\rho_{s(relative)}$ (%)	Δm (%)
A	1300	5	2.30	2.59	6.08	43	1.94
B	1300	5	2.16	3.18	6.08	52	3.11
C	1300	5	2.82	5.68	6.04	94	2.67
D	1300	5	2.52	4.40	6.04	73	7.50
A	1250	60	2.64	5.64	6.08	93	2.19
B	1250	60	2.44	3.13	6.08	52	3.24
C	1250	60	2.65	5.64	6.04	93	2.54
D	1250	60	2.42	3.96	6.04	65	7.22

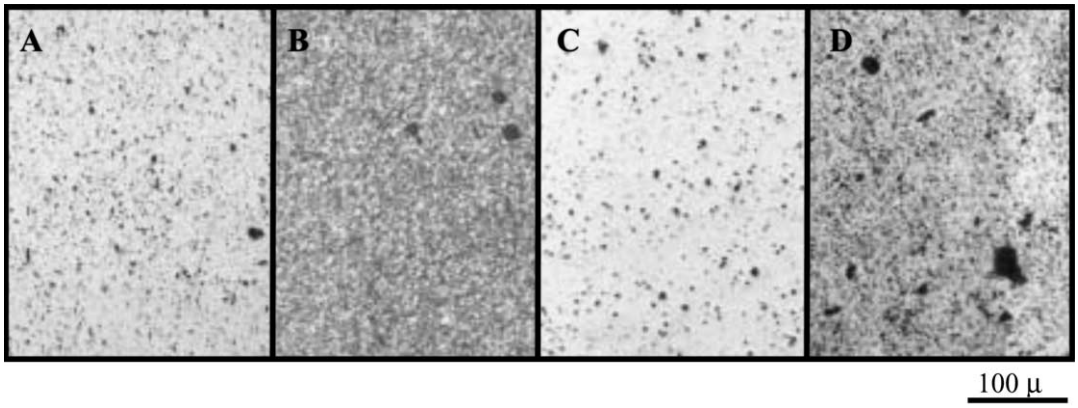

Fig. 4. Characteristic microstructures of samples A–D milled for 60 min and sintered at 1250 °C for 10 h.

distribution is most pronounced for sample D which consists of relatively dense material and areas containing large voids. A very low relative density (52%) and a porous microstructure is characteristic of sample B as well. However, in this case the pore size distribution is much narrower than in sample D. The explanation for this difference is probably that in the chromium-depleted sample more secondary phase appeared.

4. Conclusions

Reaction mixture geometry prior to the combustion (loose powder layer or compacted pellet) and (La + Ca)/Cr cation ratio in LCC to a large degree influence powder sintering behaviour. The combustion reaction mode (thermal explosion) in samples prepared in layer form results in the formation of hard agglomerates with a lower degree of reactant conversion. Better products were obtained by the self-sustaining reaction performed in pellet form. In this case mass losses after synthesis do not exceed 2.2%, and so-called weak agglomerates are formed. The relatively high sintered density (93%) of sample A, despite its stoichiomeric chromium content, was achieved due to agglomerate size reduction and consequently easier liquid phase penetration along LCC grain boundaries.

References

1. Yokohawa, H., Sakai, N., Kawada, T. and Dokiya, M., Chemical thermodynamics consideration in sintering of $LaCrO_3$-based perovskite. *J. Electrochem. Soc.*, 1991, **138**(4), 1018–1027.
2. Sakai, N., Yokohava, H., Kawada, T., Dokiya, M., Kojima, I. and Iwata, T., Sinterability and electrical conductivity of calcium-doped lanthanum chromites. *J. Mater. Sci.*, 1990, **25**, 4531–4534.
3. Bates, J. L., Chick, L. A. and Weber, W. J., Synthesis, air sintering of lanthanum and yttrium chromites and manganites. *Solid State Ionics*, 1992, **52**, 235–242.
4. Morelli, M. R. and Brook, R. J., Combustion synthesis of $LaCrO_3$ powders. *Ceramic Transactions*, 1995, **51**, 81–85.
5. Varma, A. and Lebrat, J. P., Combustion synthesis of advanced materials. *Chemical Engineering Science*, 1992, **47**, 2179–2194.
6. Zupan, K., Kolar, D. and Marinšek, M., Influence of citrate-nitrate reaction mixture packing on ceramic powder properties. *J. of. Power Sources*, 2000, **86**, 417–422.
7. Kingsley, J. J. and Pederson, L. R., Combustion synthesis of perovskite $LnCrO_3$ powders using ammonium dichromate. *Mater. Lett.*, 1993, **18**, 89–96.
8. Chick, L. A., Liu, J., Stevenson, J. W., Armstrong, T. R., McCready, D. E., Maupin, G. D., Coffey, G. W. and Coyle, C. A., Phase transitions and transient liquid-phase sintering in calcium-substituted lanthanum chromite. *J. Am. Ceram. Soc.*, 1997, **80**(8), 2109–2120.
9. De Villiers, J. P. R., Mathias, J. and Maun, A., Phase relations in the system CaO–chromium oxide–SiO_2 in air, and solid solution relations along the Ca_2SiO_4–$Ca_3(CrO_4)_2$ join. *Trans. Inns. Min. Metal, Sect. C*, 1987, **96**, C55–C62.
10. Smolej, V., Pejovnik, S. and Kaysser, W. A., Rearrangement during liquid-phase sintering of large particles. *Powder Metall. Int.*, 1982, **14**, 34–36.